sustainability

MDPI

Article

Soil Slope Instability Mechanism and Treatment Measures under Rainfall—A Case Study of a Slope in Yunda Road

Yuqiong He [1], Bo Li [1,*] and Xuan Du [2]

[1] Faculty of Transportation Engineering, Kunming University of Science and Technology, Kunming 650500, China
[2] Jinan Urban Construction Group, Jinan 250000, China
* Correspondence: m18800421151@163.com; Tel.: +86-18800421151

Abstract: The unique geological conditions in Yunnan make it likely for landslides to occur there. For the purpose of exploring the soil slope instability mechanism, this paper takes a slope in Yunda Road, Chenggong, Kunming, as case study and establishes a slope model utilizing FLAC 3D coupled with Geo-studio software. The displacement, strain and deformation rate of the slope under the condition of rainfall are simulated, and the influence of rainfall and rainfall duration on rainfall infiltration is analyzed. The results indicated the following: (1) The effective stress on and shear strength of slope soil at the foot of the slope gradually decreased under rainfall, resulting in the loosening of the slope soil and slip at the foot of the slope. This affected the stability of the upper slope which, in turn, reduced the stability of the whole slope; (2) When the duration of rainfall reached 72 h, the slope stability coefficient Fs = 0.88, indicating a failure state. The increments of principal stress and shear stress at the foot of the slope were the largest, and the strain speed was the fastest, with the maximum values of principal stress and shear stress reaching 0.412 and 0.579, respectively; (3) The maximum total displacement was 2.177 m at the foot of the slope, the maximum vertical Z-axis displacement was 1.673 m in the negative direction of the Z-axis, and the soil at the foot of the slope was 0.6 m in the positive direction of the Z-axis. Our simulation results were consistent with the actual failure of the slope. After analyzing the slope mechanism and adopting targeted treatment measures, the slope was subjected to four rainfall cycles without any sign of landslips, indicating that the effect of our interventions was favorable.

Keywords: under rainfall; soil slope; instability mechanism; treatment measures

check for updates

Citation: He, Y.; Li, B.; Du, X. Soil Slope Instability Mechanism and Treatment Measures under Rainfall—A Case Study of a Slope in Yunda Road. *Sustainability* **2023**, *15*, 1287. https://doi.org/10.3390/su15021287

Academic Editor: Antonio Miguel Martínez-Graña

Received: 16 November 2022
Revised: 22 December 2022
Accepted: 28 December 2022
Published: 10 January 2023

Copyright: © 2023 by the authors. Licensee MDPI, Basel, Switzerland. This article is an open access article distributed under the terms and conditions of the Creative Commons Attribution (CC BY) license (https://creativecommons.org/licenses/by/4.0/).

1. Introduction

At present, rainfall–slope stability is a research hotspot. Using GDEMRU software and genetic algorithms, Zhang Xinwei et al. [1] analyzed the degree of rainfall infiltration in slope soil, calculated the strength of slope soil using a strength reduction algorithm, and analyzed several slope disasters. Using Geo-Studio software, in the present study, soil slope stability and the degree of slope infiltration under rainfall conditions are analyzed. Rainfall strength and duration have a great influence on slope stability. With long duration or high intensity rainfall, the infiltration capacity of slope soil increases, reducing its stability over time [2–6]. Through a coupling analysis using ANSYS and FLAC3D software, the effects of rainfall strength on slope soil infiltration and slope stability were analyzed by Huang Ganghai [7]. Those authors pointed out that when the amount of rainfall is greater than the infiltration capacity of the slope soil, additional rainfall has a decreasing influence on slope stability. In the process of rainfall infiltration, a transient saturation zone will form in slope soil; this can only be realized by rainfall of high intensity and long duration. The transient saturation zone has a great influence on fluctuations in the groundwater level, thus affecting the overall safety and stability of the slope [8,9]. Wu Lizhou et al. [10] analyzed slope safety by applying an equal fluid dynamics governing equation combined with rainfall strength

and other factors. The results demonstrate that shallow slope soil is more sensitive to changes in rainfall strength. Nian, Gengqian et al. [11] took into account rainfall conditions and established a numerical model of unsaturated slope seepage, finding that the overall stability of a slope is not significantly affected by rainfall strength, but rather, that shallow slope soil is sensitive to changes thereof. Through a field investigation and numerical software simulation, Khan Kaleem Ullah Jan et al. [12] analyzed the change law of slope stability under the condition of rainfall, noting that rainfall reduces the gradient of slope and accelerates the infiltration rate of rainfall, which lead to an obvious lag effect of slope instability and positive pore water pressure. Ding Wenjie [13] and Zhu Lei et al. [14] used the MIDAS DTS NX software to analyze the influence of slope ratio and other factors on slope stability. Through a comparative analysis, those authors found that with an increase of slope ratio, slope stability was reduced. He Fan et al. [15] used the soil ground around the Ping 'a Highway in Qinghai Province as a case study to analyze the stability of soil slope under rainfall condition. The results revealed that changes in slope stability were greatly influenced by rainfall strength and the soil parameters. In this paper, taking the soil slope on Yunda Road as an example, the mechanism of slope instability under rainfall is studied by numerical analysis. On the bases of previous research and the geographical environment of the study site, treatment measures for this slope are proposed.

2. Overview of Study Site

The study site is located on the right side of Yunda Road (when driving toward Wanxichong) in Chenggong District, Kunming (E102 51′ 47.27″ and N24 49′ 39.44″). The area is in the north subtropical zone with a low latitude plateau/monsoon climate. The average annual temperature is 14.7 °C and the average annual rainfall is 789.6 mm; 80% of the annual rainfall occurs in the period from April to October. The study site is an east–west, north-back shady slope, within which Slopes I, II and III have a slope rate of 1:1, while Slope IV has a slope rate of 1:1.2. The total length of the slope along the driving direction (toward Wanxichong) is about 260 m, and the slope height is about 40 m. Slope I is paved with mortar rubble (10 cm thick) with no retaining wall at its foot. Slopes II, III and IV are protected by mortar diamond grids and grass. The soil is dominated by silty clay, and the vegetation at the top of the slopes is mostly low shrubs, with a few trees and no heap loading. A work side three-dimensional terrain map and study area map are shown in Figures 1 and 2, respectively.

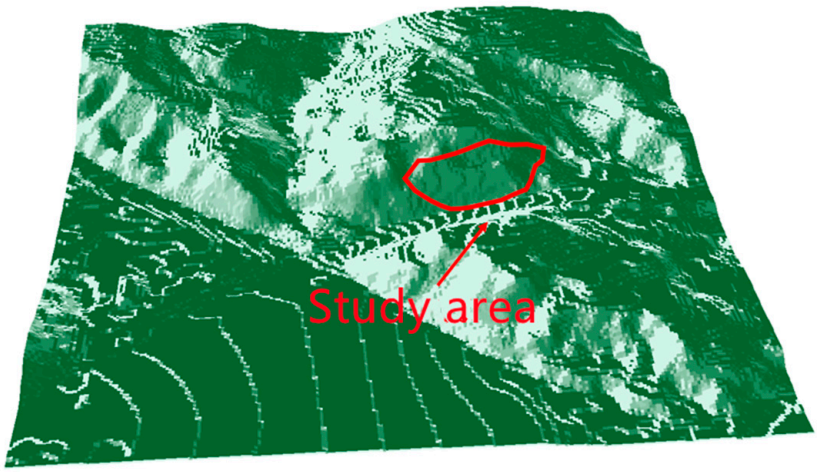


Figure 1. Three-dimensional topographic maps.



Figure 2. Study area map.

3. Slope Modeling Analysis

3.1. Slope Calculation Theory

3.1.1. Limit Equilibrium Method

According to the unstructured soil shear strength theory and the limit equilibrium method put forward by Fredlund. assuming that the slope is parallel to the bedrock surface, the slope stability coefficient can be calculated by Formula (1). If the sliding resistance force of slope is equal to that of sliding force, the slope is in the limit equilibrium state,

$$F_S = \frac{c' + (\sigma_n - \mu_a)\tan\varphi' + (\mu_a - \mu_w)\tan\varphi^b}{\gamma z_w \cos a \sin a} \tag{1}$$

where c' is effective cohesive force; φ' is effective friction angle; $\sigma_n - u_a$ is normal stress; $u_a - u_w$ is matric suction; φ^b is the friction angle corresponding to the contribution of matric suction to shear strength; γ is slope soil natural density; z_w is the vertical thickness from the wet peak to the surface; and α is the gradient angle.

3.1.2. Strength Reduction Method

The strength reduction method is employed to calculate and judge the stability of slope soil, whose advantage is that the stability coefficient of the slope can be directly calculated without assuming the form and position of the slip surface in advance, and the gradual failure process of the slope can be simulated. In this method, the shear strength indexes c and φ of soil are continuously reduced through repeated iterative computations. When c and φ are reduced to a certain value of c' and φ' (in Formula (2)), the slope soil instability occurs, and the reduction multiple of k is the stability coefficient.

$$\begin{gathered} \tau' = \frac{\tau}{k} = \frac{c+\tan\varphi}{k} = c' + \tan\varphi' \\ c' = \frac{c}{k} \end{gathered} \tag{2}$$

where $\varphi' = \arctan(\frac{\tan\varphi}{k})$.

Convergence principle of iterative calculations is that unbalanced nodal force is less than the specified precision, that is:

$$\begin{gathered} \frac{\left[\sum_{i=1}^{n}(\psi_i)^2\right]^{\frac{1}{2}}}{\left[\sum_{i=1}^{n}(P_i)^2\right]^{\frac{1}{2}}} < \varepsilon \\ \psi_i = F\delta_i - P_i = \iint_e B^T D_i \varepsilon_i dV - P_i \end{gathered} \tag{3}$$

where n is number of degrees of freedom;γ is iterative time;ε is specified precision; ψ_i is unbalanced nodal force vector; $F\delta_i$ is the node force vector; P_i is point load vector of section; ε_i is the element stress vector; D_i is element stiffness matrix;B^T is element transpose matrix; V is volume; and e is a unit.

3.2. Slope Model Establishment

According to the slope topography, the slope model (Figure 3) is established and analyzed as follows:

1. Slope model is calculated and analyzed by Mohr–Coulomb model, which is based on shear strength theory as failure standard and is suitable for slope safety stability analysis of soil.
2. The left and right water head heights of the model are set to 15 m and 10 m, respectively; the three-dimensional model has a horizontal distance of 94 m and a vertical distance of 50 m, in which 34,864 grid cells and 44,532 nodes are set in the model. The slope is divided into three soil layers from top to bottom, namely silty clay layer, clay layer and metamorphic rock layer.
3. FLAC3D software can accurately calculate the initial stress analysis of the slope, and the initial slope stress has great influence on the seepage and displacement change of the slope. To obtain accurate analysis data, FLAC3D software should be utilized to analyze the stress distribution under the initial slope stress. Calculate slope displacement and slope safety and stability coefficient, then output the analysis results to Geo-studio receiving format, including the rainfall data, and further analyze the change characteristics of seepage field and slope displacement under rainfall slope infiltration.
4. Slope monitoring focuses on slope toe at all levels, so one monitoring point is set at slope toe at all levels. The seepage situation is shown by the cloud picture of the monitoring point, and the displacement and stress strain are shown by the vector cloud picture. The seepage and stress strain of the slope are analyzed.

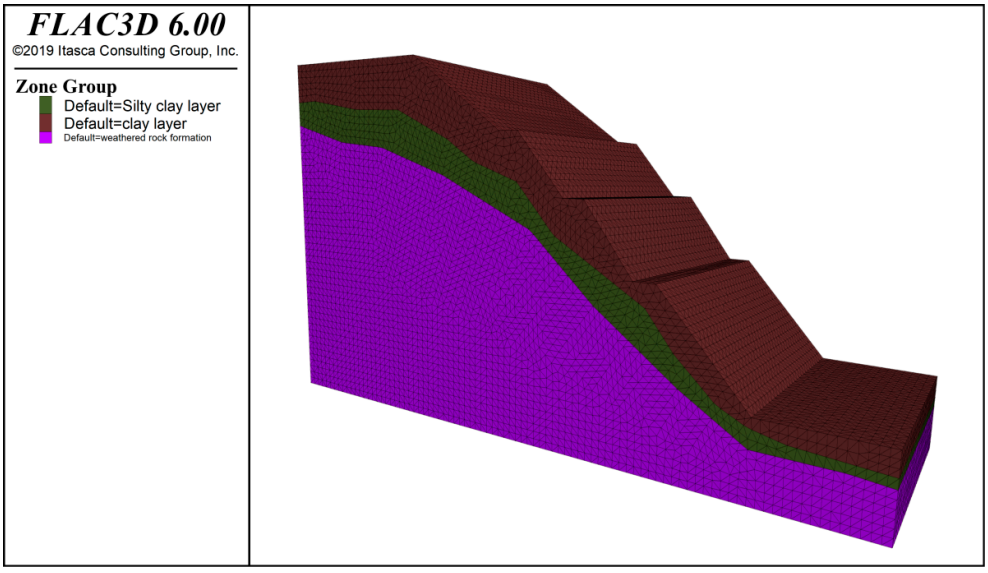


Figure 3. Slope model.

3.3. Slope Model Establishment

On 10–12 June 2015, the persistent rainfalls were 60 mm/d, 82 mm/d and 735 mm/d, respectively. The total rainfalls in three days were 273 mm, accounting for 75.8% of the rainfalls in June, July and August, respectively, for three months. Based on the aforementioned rainfall data, the stability of the slope is simulated and calculated, the slope instability mechanism is analyzed, and the corresponding treatment scheme is put forward. According to geological prospecting data, the physical and mechanical parameters of this slope soil are shown in Table 1.

Table 1. Soil parameters.

	Natural Bulk Density (kN/m^3)	Modulus of Elasticity (MPa)	Poisson's Ratio	Cohesive Strength (kPa)	Inner Friction Angle (°)
Silty clay	18.8	2.69	0.25	11.6	20.5
Clay	19.6	4.11	0.28	15.8	27
Metamorphic rock layer	34	5.48	0.35	19.2	31

4. Rainfall Infiltration and Stability Analysis

4.1. Pore Water Pressure Analysis

According to the situation of rainfall from 10–12 June 2015, Geo-studio software was applied for transient simulation analysis of slope pore water pressure, as shown in Figure 4. With the increase in rainfall duration, the pore water pressure in the unsaturated zone of the slope changes. In the process of rainfall lasting for 72 h, due to the influence of groundwater level, the pore water pressure at the foot of the slope, which is higher than the water level line, changes greatly due to the capillary water pressure in the slope. The pore water pressure changes little when the slope foot is close to the groundwater level. With the continuous development of rainfall infiltration, the water content of slope soil increases, especially the accumulated water at the foot of the slope is obviously more than that on the uphill slope, which reduces the absolute value of negative pore water pressure and dissipates matric suction. This results in the gradual decrease in effective stress and shear strength of the slope soil at the foot of the slope, thereby causing slope soil loosening and slipping at the foot of the slope, and extending to the upper Slope I, thus reducing the safety and stability of the whole slope.

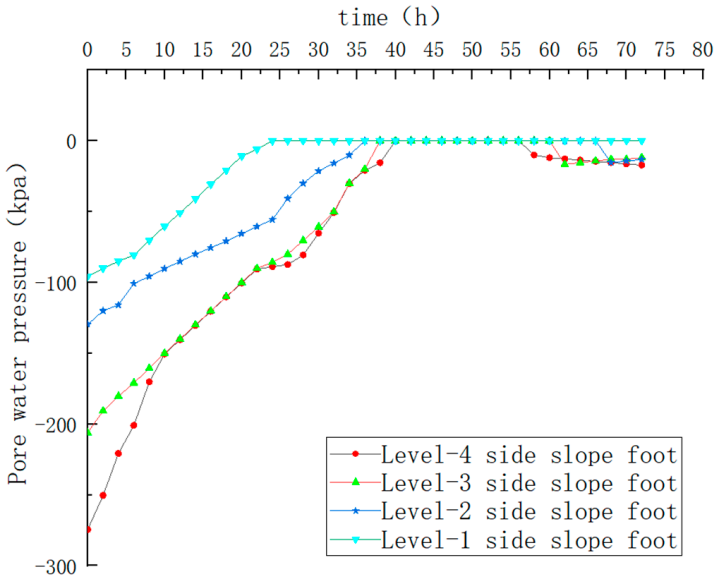


Figure 4. Pore water pressure diagram.

4.2. Saturation Analysis

Under the action of rainfall, with the continuous increase in rainfall time, the saturation variation trend of each slope foot of the rock-soil slope is shown in Figure 5. Slope I has the shortest saturation time at the foot of the slope, because it is close to the groundwater level, and the slope soil below the groundwater level is saturated by default. The way of rock slope soil rainfall infiltration from the monitoring point to the groundwater level is short, so the saturation time is short, and the rock slope soil stays saturated for a long time. At the foot of the fourth slope, the elevation is high, and the slope soil of rock keeps infiltrating in the process of rainfall. In the process of rainwater infiltration, it shows that

the greater the intensity of rainfall, the longer the duration of rainfall, and the more obvious the change range of saturation. Therefore, in the process of rainfall, regardless of the pore structure of rock slope soil and the position of groundwater level, the change in rock slope soil saturation is the joint effect of rainfall strength and rainfall duration. After the slope soil is saturated and softened, the increase in pore water pressure and saturation leads to the decrease in cohesion and effective stress of the slope soil. Therefore, rock slope soil will have large settlement deformation in the consolidation process. In addition, after slope soil reaches saturation, saturated soil may also have seepage phenomenon, leading to failure in the slope soil skeleton.

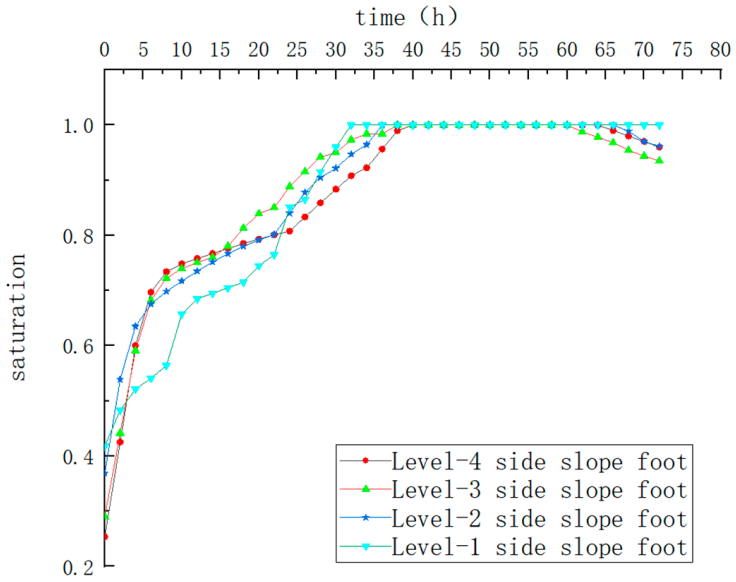


Figure 5. Saturation diagram.

4.3. Slope Displacement and Strain Simulation

Using rainfall data from 10–12 June 2015, the displacement vector of the slope was calculated by strength reduction method, as shown in Figure 6. The maximum displacement deformation of the slope occurred at the foot of the slope, and the deformation rate was fast, and the displacement amount was large.

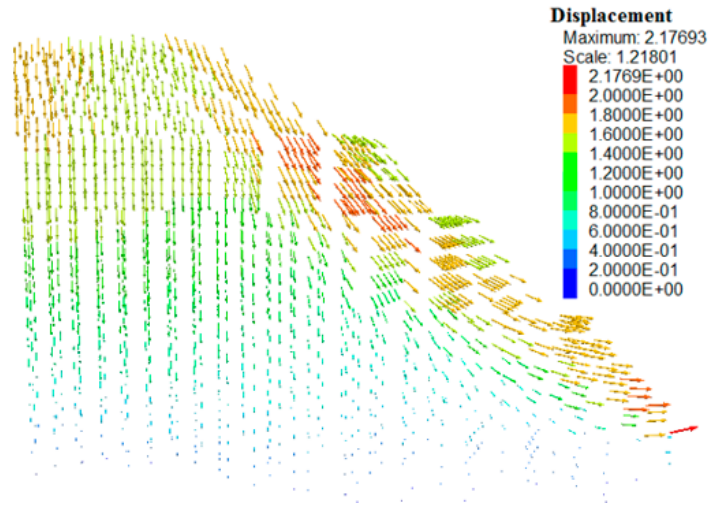
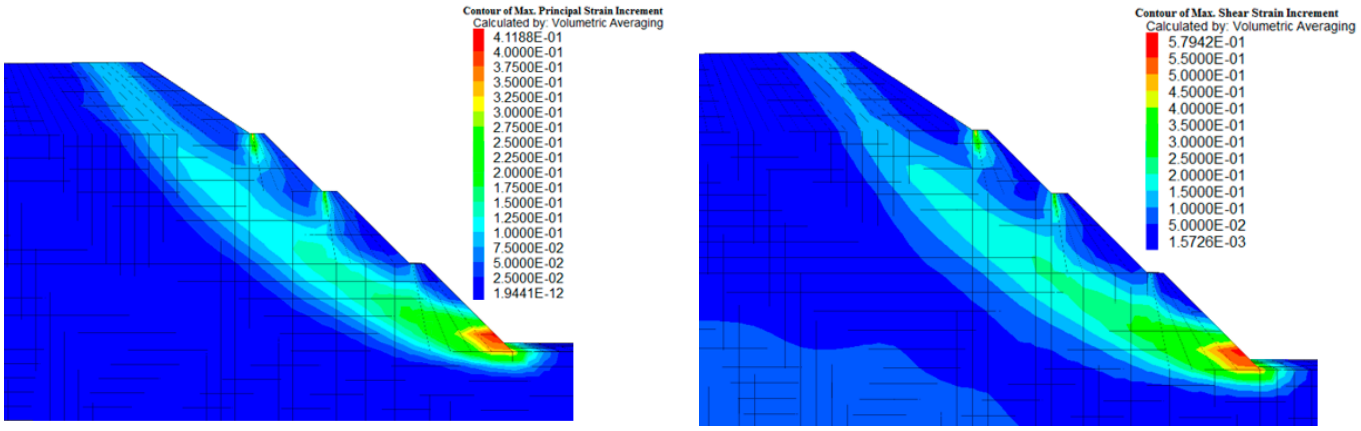


Figure 6. Displacement vector diagram.

① At the foot of the slope, displacement occurred at a high rate at the beginning in the X-axis direction, and subsequently gradually leveled off. In the Z-axis direction, displacement also occurred at a high rate along the negative direction of the Z-axis. Afterwards, due to the sliding and pushing action of the upper steps, the slope soil at the foot of the slope moved upward, that is, it moved positively along the Z-axis, and the displacement rate leveled off at the later stage.

② The top of the slope firstly moved in the negative direction of the X-axis and then moved in the positive direction of the X-axis. A small amount of negative displacement occurred at the top of the slope since the displacement rate at the foot of the slope was much higher than that at the top of the slope, making the top of the slope tilt backward. The overall displacement trend of the slope moved to the positive direction of the X-axis, that is, a large displacement occurred along the positive direction of the X-axis; in the direction of the Z-axis, it always moved along the negative direction of the Z-axis.

③ At the foot of the slope, the increment of principal stress and shear stress was the largest, and the strain speed was the fastest. The maximum increment values of principal strain and shear strain were 0.412 and 0.579, respectively, as shown in Figure 7. A significant plastic penetration area was formed in the slope, and any external force broke the stress equilibrium state of the slope and slid along the potential sliding surface of the plastic penetration area. The foot of the slope slid at the stress concentration, and its deformation rate was fast, and the displacement was large. The displacement at the top of the slope was mainly induced by the joint action of the displacement at the foot of the slope, whose deformation rate and displacement amount changed with the variation at the foot of the slope, and the deformation rate was smaller than that at the foot of the slope.



(**a**) (**b**)

Figure 7. Strain diagram: (**a**) maximum principal stress; (**b**) maximum shear strain.

4.4. Slope Stability Coefficient

4.4.1. Without Considering Rainfall

Due to the stress release effect after slope excavation, many small cracks are generated at the rear edge of the slope top, and with the increase in the free surface, a large-scale tensile failure crack is gradually formed, as depicted in Figure 8. Without rainfall and other load disturbances, the stability coefficient of slope calculated by limit equilibrium method is 1.03, as indicated in Figure 9. It can be seen that the slope is basically in a critical failure state without rainfall and other loads, and has a tendency of instability development, belonging to a kind of low-stability slope.



Figure 8. Pulling cracks at the back edge of the slope top.

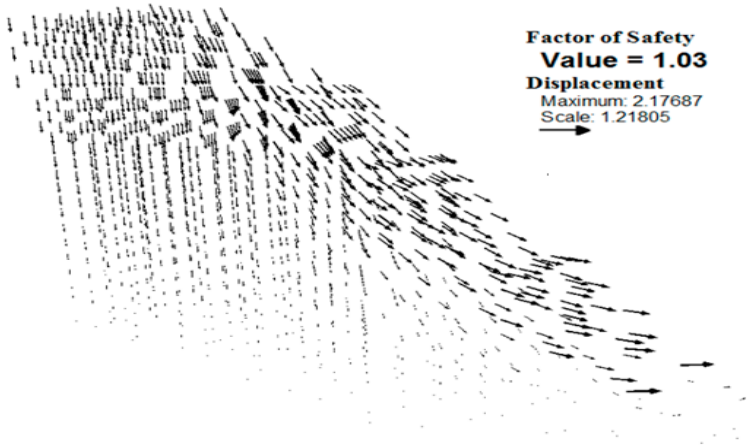


Figure 9. Stability coefficient and sliding tendency diagram.

4.4.2. Considering Rainfall

According to the data of rainfall from 10–12 June 2015, the stability of the slope was calculated, and the stability coefficient was calculated by limit equilibrium method. When rainfall lasted for 72 h, the slope stability coefficient Fs was equal to 0.88, as shown in Figure 10. Slope safety and stability coefficients all showed the law that the continuous safety coefficient of rainfall decreased, of which the difference was that the greater the strength of rainfall, the more sensitive the slope safety and stability coefficient changed. Meanwhile, the slope changed from critical failure state to dangerous collapse state. The slope produced a large-scale landslip from the 72 h rainfall to the stop of rainfall. After the stop of rainfall, the pore water pressure in the slope landslip gradually dissipated, whereas the water in the slope moved to the sliding zone, resulting in the increase in the slope weight and the gradual increase in cracks, resulting in the local stress concentration of the slope, which led to the slope sliding instability failure. Rainfall caused the slope to slide down on a large scale along the potential sliding surface, as shown in Figures 11 and 12, which demonstrated that it was reasonable to judge the slope stability and failure according to the stability coefficient.

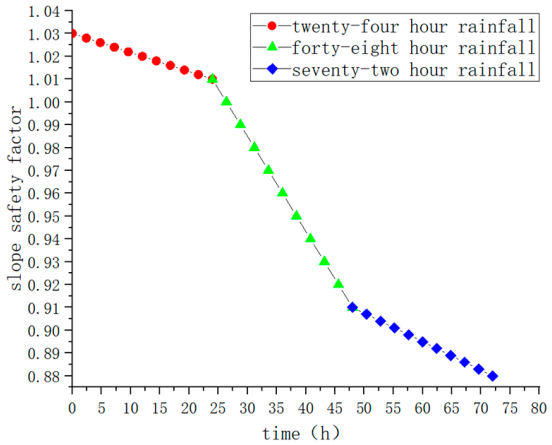


Figure 10. Variation diagram of safety factor.



Figure 11. Full picture of slope landslip.



Figure 12. Landslip in the study area.

4.5. Comparison between Actual Slide Position of Slope and Simulation Results

After the slope was excavated, a large number of cracks were produced at the rear edge of the slope top, which provided a fast passage for rainfall infiltration and accelerated the decline of slope soil. At the beginning, the first and the fourth slope toe collapsed locally. Due to the loss of the supporting function of the lower slope soil, the second and third grade slopes of the corresponding positions also declined. Eventually, a large-scale landslip instability phenomenon occurred in this slope, and its instability development process is shown in Figure 13. In the most serious part of the landslip, the rubble and rhombic grid slope protection were completely damaged, and the landslip slope soil slipped into Yunda Road for 25–30 m approximately, blocking the road leading to Wanxichong and the opposite inner lane. There were obvious tensile failure marks on the trailing edge of the landslip, and obvious shear failure marks on the sliding surface.



Figure 13. Landslip development process diagram.

According to the calculated cloud map of the slope total displacement (Figure 14), the maximum total displacement occurred at the foot of the first and fourth slopes, which was 2.177 m (Figure 14a) (3). The displacement deformation also occurred at the step of Slope IV; the maximum displacement in the Z-axis occurs at the top of the slope (Figure 14b), and the displacement in the negative direction of the Z-axis is 1.673 m. On the other hand, the slope soil at the foot of the slope had a displacement of 0.6 m along the positive direction of the Z-axis, which was because the slope soil at the foot of the slope had been raised by 0.6 m due to the downward inclination of the trailing edge of the slope soil in line with the characteristics that the front edge of the slope surface bulges outwards, leading to the rupture and damage of the rubble slope protection at the foot of the slope. The actual sliding depth and position of the site were basically consistent with the simulation results.

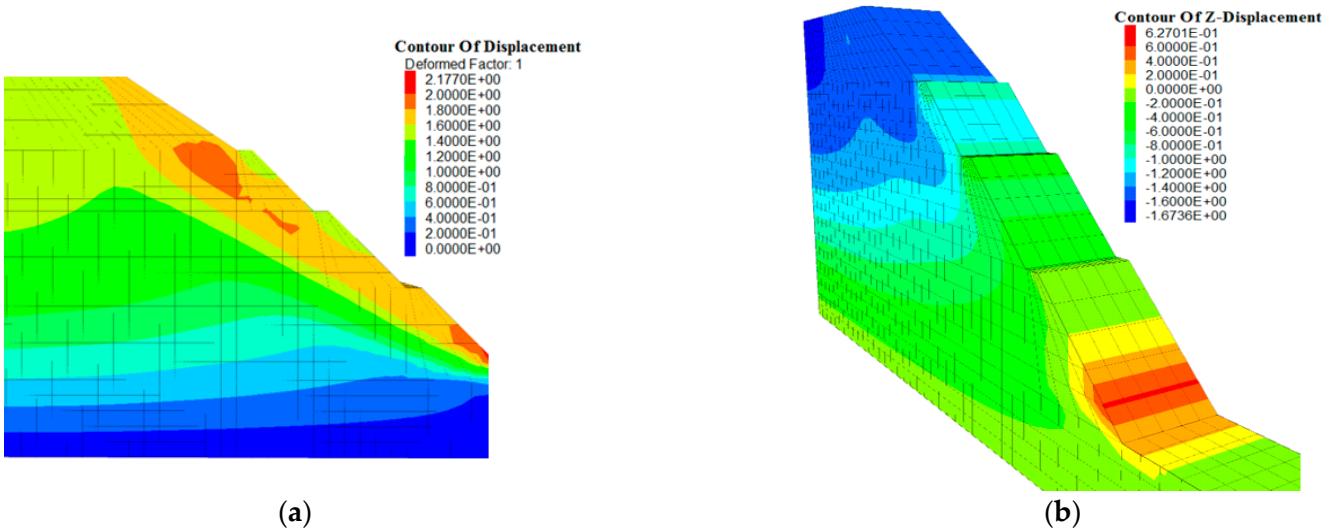


Figure 14. Displacement diagram: (**a**) general layout; (**b**) Z−direction displacement.

5. Landslip mechanism and Governance

5.1. Slope Sliding Mechanism Analysis

Combining the field investigation and simulation calculation results, it is considered that the slope sliding mechanism is as follows:

(1) The slope has experienced a long-term deformation and development process before its instability. Slip and tensile crack are two basic ways of slope deformation, which make the stress in the slope redistribute continuously, and the stress concentrated area has a repeated process of slip–tensile crack. Thereby, the landslip danger can occur only when the slope is triggered by external conditions in the process of cumulative failure.

(2) The slope excavation process broke the stress equilibrium state of the original slope body, resulting in unloading relaxation and strength weakening of the slope soil. Many cracks appeared above the slope and at the rear edge of the top of the slope, forming surface tension cracks, which provided airport conditions for the final occurrence of the landslip.

(3) The water content of the slope soil in an unsaturated zone will increase, and some unsaturated slope soil in the slope will be transformed into saturated slope soil under rainfall. This lowered the shear strength of the slope soil, so rainfall played a certain role in boosting the occurrence of slope collapse.

(4) With the continuous development of rainfall, temporary additional water pressure will be formed in some areas of slope soil on the surface of the slope, and seepage will be formed in the slope soil, resulting in the increase in pore water pressure, which will lead to the rise of groundwater level in the slope, resulting in slope failure.

(5) Slope soil of slope rock is of poor quality, leading to the mechanism of landslip evolution in the soil layer, and its mechanical mode is the evolution process of tensile-crack–shear-slip mode. Furthermore, the slope retaining wall is buckled, forming the traction landslip, which then causes the instinctive sliding of the superior slope, and finally leads to a large-scale landslip phenomenon in the slope.

5.2. Slope Stability Treatment Measures

According to the sliding mechanism and specific conditions of the slope, the slope treatment measures are mainly to enhance the shear resistance of the slope and improve the stability of the slope. The treatment measures are as follows:

(1) Drive pre-stress bolt into the tension crack at the rear edge of slope and reduce the appearance of airport surface to decrease the contribution of crack to slope collapse.

(2) Cut the slope to clear the sliding slope soil. According to the position of the sliding surface, gradually remove the landslip slope soil from top to bottom and remove all the slope soil with cracks above the slope excavation line.

(3) Reduce the height of each grade of slope and slow down the gradient. A 5-grade slope rate is adopted, with the first grade of the slope being between 1: 1.1 and 1: 1.2, and the second grade to fifth grade of the slope being between 1: 2 and 1: 2.5, so as to ensure a smooth transition among all grades of slopes.

(4) Set intercepting and drainage ditches. Set intercepting ditch at the periphery of the slope excavation line, set a drainage ditch on each falling platform, and set a drainage ditch along the slope direction to remove rainwater and surface water collected by surface runoff, and discharge them into a roadside drainage ditch to prevent rainwater from entering the slope soil.

(5) Slope soil consolidation protection. The slope protection in the form of a cast-in-place concrete frame beam and bush slope protection is adopted. The frame beam can strengthen the whole slope, and the low shrubs with developed roots are planted in the frame to stabilize the surface soil.

(6) Set an anti-slide retaining wall. Cast-in-place concrete anti-slide retaining walls are set at the slopes at all levels to reinforce the slopes at all levels.

After calculation, the safety factor of the slope after treatment is 1.293. After four rainfall cycles, the slope shows no signs of landslip, indicating that the treatment measures of the slope are feasible and effective. The slope after treatment is shown in Figure 15.



Figure 15. Slope after treatment.

6. Discussion

(1) The main reason for this slope instability is the nature of the slope itself under rainfall conditions. The soil of the slope is mainly silty sand, and the property of rock slope soil is soft rock and soil, with loose structure and poor bonding condition, and it produces an obvious sense of depression when stepping on it. The weak and high plasticity of rock slope soil is one of the main causes of landslip. The low shear strength, integrity and weak cohesiveness of slope soil directly lead to the deformation and failure of the slope.

(2) Owing to the weak nature of the slope soil, small-scale failure and some large-scale failure precursors appeared in the early stage of the slope, such as slope cracking and small-scale collapse, and finally the slope soil medium in the under rainfall sliding zone was gradually damaged. Once the external load was greater than the maximum value that the critical state could bear, the slope soil on the potential sliding surface will break away from the parent slope and slide along the sliding surface to a position with low binding force, resulting in displacement deformation and large-scale sudden instability.

(3) In the original design, the slope adopts the slope protection method of prismatic lattice and grass planting, and there is no retaining wall at the foot of the slope. This protection method can only stabilize the surface slope soil but is not enough to support the stability of the deep slope soil, and the problem of slope rainwater infiltration has not been solved. Under the action of various external factors, a potential sliding surface will be formed. Under the action of rainwater infiltration, the weight of the upper sliding body is increased, which leads to the increase in the sliding force of the landslip body, which is not conducive to the stability of the slope.

7. Conclusions

(1) The rainfall during 10–12 June 2015 was the direct cause of this landslip, and the front edge of the slope produced a compression shear sliding surface. The porosity and water permeability of soft rock slope soil are large, and it is easy to infiltrate after rainfall, and there are no centralized drainage facilities. The slope protection and waterproof and drainage effects are poor, resulting in serious infiltration of the slope soil, which leads to a serious increase in slope soil, especially at the foot of the slope, and a decrease in cohesive force, which greatly reduces slope stability and integrity. Under the action of rainfall infiltration, a large-scale instability failure phenomenon occurs.

(2) Through the dynamic analysis of rainfall, slope stability and time, it can be seen that the initial stage of strong rainfall is the time period when the slope safety factor decreases fastest. At this time, the surface slope soil in the slope is rapidly saturated, which increases the sliding force at the front edge of the slope and forms a seepage field in the slope. Under the action of seepage force and hydrodynamic pressure, a traction multistage landslip failure is formed, which accelerates the slope instinctive sliding.

(3) The slope instability is closely related to the nature of slope soil and the orientation of slope surface accordingly. The slope soil of slope rock has loose structure, poor bonding condition and a shady slope surface, so that the water content in slope soil is high, and its shear resistance is reduced, which directly leads to slope sliding.

(4) In terms of the treatment of landslip slope, it is suggested to slow down the slope proportion, set a gravity retaining wall at the foot of the slope and fix the surface soil with concrete frame beams and shrubs for slope protection. It is also suggested to build an anti-slide retaining wall at the foot of each Slope I to reinforce slope soil at all levels, build intercepting ditches outside the excavation line at the top of the slope and on each level of broken platform (anti-slide retaining wall) to remove surface water and collect water from the slope, and take corresponding drainage measures to remove groundwater and reduce the impact of rainwater on the slope, which can ensure the stability of the slope.

(5) The slope surface is covered with bush vegetation, which can reduce the erosion of rainwater, reduce the amount of rainwater seeping into the slope soil, and play the role of rainfall river closure. The root system of bush vegetation can also reinforce the slope soil on the rock surface. The slope has gone through three rainfall cycles, and the slope has no sign of landslip, which indicates that the treatment measures of the slope are feasible and effective.

Author Contributions: Conceptualization, methodology, formal, and writing—original draft, B.L.; conceptualization, methodology, supervision, writing—review and editing, Y.H.; conceptualization, methodology, supervision, writing—review and editing, X.D. All authors have read and agreed to the published version of the manuscript.

Funding: This research was funded by the "National Natural Science Foundation of China Projects, grant number 41807258" and "Yunnan Province Talent Development Project, grant number KKSY201406009" and the Project of the Transportation Department of Yunnan Province (Yunjiao Science and Education Convenience No.4 [2022]).

Data Availability Statement: Not applicable.

Conflicts of Interest: The authors declare no conflict of interest.

References

1. Zhang, X.W.; Zhu, X.G.; Feng, C. Inversion analysis of geotechnical parameters of Wangjiatai Landslide based on rainfall infiltration generalization model. *Sci. Technol. Eng.* **2022**, *22*, 3485–3490.
2. Li, C.; Cai, L.M. Influence of initial seepage field on rainfall infiltration characteristics and stability of slag slope. *Chin. J. Civil Environ. Eng.* **2021**, *43*, 1–9. (In Chinese)
3. Hong, Z.Y.; He, Y.Q.; Li, M. Different rainfall conditions of unsaturated seepage flow under the action of large soil field stability analysis. *J. Min. Res. Dev.* **2021**, *9*, 101–106. [CrossRef]
4. Kang, X.P.; Meng, F.C.; Zeng, C. Slope stability under the condition of heavy rainfall and soil field course analysis. *Highway* **2019**, *33*, 34–39. [CrossRef]
5. Wu, Z.B.; Wang, C.Q.; Zeng, J.B. Numerical simulation analysis of seepage flow and stability of slope soil under different rainfall intensities. *Saf. Environ. Eng.* **2017**, *24*, 148–153. [CrossRef]
6. Yuan, H.; Xie, K.; Lan, H. Highway (guizhou) and abandon soil in slope stability analysis. *J. Water Resour. Hydropower Technol. Gansu Prov.* **2020**, *56*, 40–43. [CrossRef]
7. Huang, G.H. Stability analysis of dump in complex terrain under heavy rainfall infiltration. *Chin. J. Geotech. Eng.* **2013**, *35*, 292–295. (In Chinese)
8. Fu, H.Y.; Zeng, L.; Jiang, Z.M. Highway slope under the condition of rainfall transient saturated zone development rule. *China J. Highw. Transp.* **2012**, *25*, 59–64. [CrossRef]
9. Zeng, L.; Shi, Z.N.; Fu, H.Y. Rainfall infiltration on the slope the influence of transient saturated zone distribution. *China J. Highw. Transp.* **2017**, *30*, 25–34. [CrossRef]
10. Wu, L.Z. Analytical solution of rainfall infiltration for vegetated slope in unsaturated soils considering hydro-mechanical effects. *Catena* **2022**, 217. [CrossRef]
11. Nian, G.Q. Rainfall infiltration boundary conditions and stability of a fractured-rock slope based on a dual-continuum model. *Hydrogeol. J.* **2022**, *30*, 829–847. [CrossRef]
12. Khan, K.U.J. Influence of rainfall infiltration on the stability of unsaturated coal gangue accumulated slope. *J. Mt. Sci.* **2021**, *18*, 1696–1709. [CrossRef]

13. Ding, W.J.; Ma, X.P.; Peng, Y.H. Sensitivity analysis of factors affecting stability of highway dump slope. *Shan Dong Land Resour.* **2022**, *38*, 82–88.
14. Zhu, L.; Hong, B.N. Sensitivity analysis of influencing factors of shallow landslide of coal measure soil. *J. Yangtze River Sci. Res. Inst.* **2011**, *28*, 67–71, 75.
15. He, F.; Yin, J.; Chen, Z.W. Qinghai province highway natural rainfall experimental research on soil erosion and soil field. *Bull. Soil Water Conserv.* **2008**, *02*, 131–134. [CrossRef]

Disclaimer/Publisher's Note: The statements, opinions and data contained in all publications are solely those of the individual author(s) and contributor(s) and not of MDPI and/or the editor(s). MDPI and/or the editor(s) disclaim responsibility for any injury to people or property resulting from any ideas, methods, instructions or products referred to in the content.